



HAL
open science

Assessing the Firing of Ceramic Materials: a Seriation-Based Approach

Nicolas Frerebeau

► **To cite this version:**

Nicolas Frerebeau. Assessing the Firing of Ceramic Materials: a Seriation-Based Approach. 2024. hal-04388590

HAL Id: hal-04388590

<https://hal.science/hal-04388590>

Preprint submitted on 11 Jan 2024

HAL is a multi-disciplinary open access archive for the deposit and dissemination of scientific research documents, whether they are published or not. The documents may come from teaching and research institutions in France or abroad, or from public or private research centers.

L'archive ouverte pluridisciplinaire **HAL**, est destinée au dépôt et à la diffusion de documents scientifiques de niveau recherche, publiés ou non, émanant des établissements d'enseignement et de recherche français ou étrangers, des laboratoires publics ou privés.



Distributed under a Creative Commons Attribution 4.0 International License

Assessing the Firing of Ceramic Materials: a Seriation-Based Approach

Nicolas Frerebeau^{1,*}

Accepted for publication on 2023-09-15

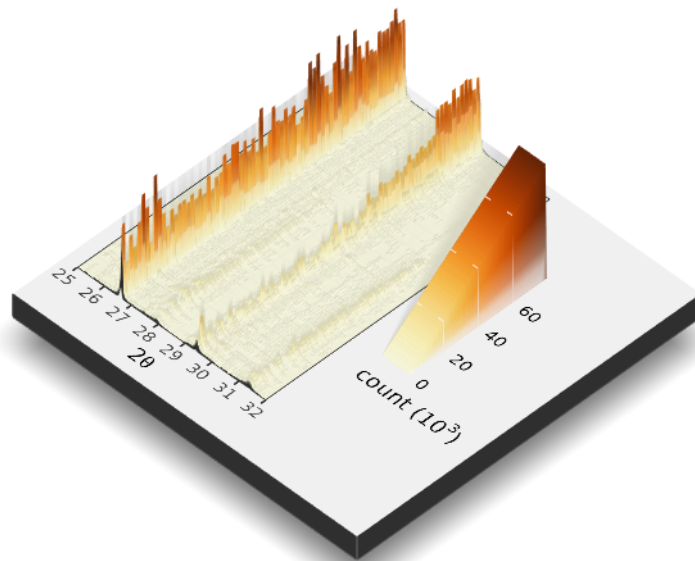
Abstract

The study of the firing of archaeological ceramics is a key factor in interpreting ancient techniques and related social practices. This study proposes a new method based on the correspondence analysis of powder X-ray diffraction data (XRD), aiming to provide an alternative to the so-called Equivalent Firing Temperature framework. The properties of correspondence analysis and its application for matrix seriation enable the description of the firing of a ceramic assemblage. The application of correspondence analysis to XRD data of Iron Age ceramics revealed the significant potential of this statistical method in the technological analysis of ancient pottery. This allows to order a large number of samples according to a firing gradient and to track mineralogical transformations occurring during firing. This method should let to more precise comparisons than those based on estimating the equivalent firing temperature.

¹ UMR 6034 Archéosciences Bordeaux

* Correspondence: Nicolas Frerebeau <nicolas.frerebeau@u-bordeaux-montaigne.fr>

Keywords: X-ray diffraction; ceramic firing; correspondence analysis; matrix seriation



License

This work is licensed under a Creative Commons Attribution 4.0 International License.

Change record

Version	Date	Description	DOI
1.0	2023-06-09	Submitted to <i>Archéosciences</i>	10.5281/zenodo.8020138
1.1	2023-08-01	Corrections based on reviews	10.5281/zenodo.8204409
1.2	2023-09-15	Accepted for publication	10.5281/zenodo.10492776

1 Introduction

Firing is a “strategic step” (Lemonnier, 1983) of the ceramic production process: its success largely determines the final mechanical, refractory and — to some extent — aesthetic properties of the artifacts. Moreover, in case of failure this step involves the risk of losing all or part of the load to be fired and the associated human labor time. The study of the firing of archaeological ceramics is thus a key factor in interpreting ancient techniques and related social practices. In this regard, significant methodological research has been carried out since the pioneering work of Shepard (1936), leading to the widespread use of the so-called *Equivalent Firing Temperatures* (EFT) as a way to describe the firing of archaeological ceramics (Tite, 1969a ; Tite, 1969b). The EFT is a point estimator tied to standard experimental conditions, defined as “the temperature maintained for one hour which would produce the observed mineralogy or microstructure” (Tite, 1995).

The EFT is undoubtedly practical, but it raises several methodological and conceptual problems. A full review is beyond the scope of this study (see Frerebeau & Pernot, 2018 for a detailed discussion), but two points can be made. On the one hand, EFT creates unnecessary ambiguity about the real firing temperature. Tite (1995 ; 1999) points out that the EFT does not account for the temperature within the firing structure. At best, it serves as an indication of the heat transmitted during the firing process that led to the observed transformations (mineralogical or microstructural), i.e., a combination of temperature and time. On the other hand, Gosselain (1992) and Livingstone Smith (2001) have highlighted the limitations of this framework. EFT alone does not provide a precise understanding of the firing conditions or the specific firing techniques employed.

Therefore, this study proposes a new method based on the multivariate analysis of powder X-ray diffraction (XRD) data, aiming to provide an alternative to the EFT framework. This method follows the principle of parsimony and has two main objectives: (1) to avoid the use of external references, whether experimental or ethnographic data; (2) to construct the simplest possible model by limiting the number of hypotheses involved.

XRD is routinely used to investigate the mineralogical composition of archaeological ceramic bodies. Typically, XRD is employed qualitatively, focusing on identifying mineralogical phases that have formed during firing, for understanding the firing history and the transformations that occurred within the ceramic material. Quantitative analysis of XRD data faces significant difficulties due to the multiphase nature, poor crystallization, and amorphous content of archaeological ceramics. Estimating quantitative mineralogical compositions through methods like the RIR method (Hubbard & Snyder, 1988) or Rietveld refinement (Rietveld, 1969) is a challenging and highly skilled exercise, requiring in-depth knowledge of the material.

Limited work has been done on the use of multivariate methods for the analysis of X-ray diffraction data from archaeological materials. Different approaches have been used such as Linear Discriminant Analysis (Garcia Jimenez *et al.*, 2006), Principal Component Analysis (de la Villa *et al.*, 2003 ; Holakoei *et al.*, 2014) or hierarchical clustering (Piovesan *et al.*, 2013 ; Maritan *et al.*, 2015), mainly for classification purposes.

In this study, we show that correspondence analysis (CA) of X-ray diffractograms can be used to assess the firing of ceramic materials. The properties of correspondence analysis and its application for matrix seriation enable the description of the firing of a ceramic assemblage and identification of outliers. Calibration data sets can be produced solely based on archaeological evidence to assess ceramic firing practices, eliminating the need for laboratory references. To illustrate this method, we examine XRD data of Iron Age ceramics from the Mas de Moreno workshop (Teruel, Aragon, Spain).

2 Material and method

2.1 Archaeological samples

Sampling was carried out in such a way that each sample was taken from a single artifact. Particular attention was paid to the risk of contamination by systematically discarding sherds that had been glued back together or that had undergone any chemical treatment.

59 ceramics from the Mas de Moreno workshop (Foz-Calanda, Teruel, Aragon; table 2) were sampled to

represent the entire period of the workshop’s activity (Frerebeau, 2015a ; Frerebeau *et al.*, 2020). The workshop was active between 225-200 BC and 40-30 AD. Previous archaeological studies of the workshop have highlighted three successive phases of activity, characterized by changes in the productive space and the emergence of Roman elements (Gorgues & Benavente Serrano, 2007 ; Gorgues & Benavente Serrano, 2012). Several kilns have been excavated, with discontinuation and destruction occurring around 50-40 BC (Gorgues & Benavente Serrano, 2012). The use of a larger amphora kiln, the production of Roman amphorae, and the presence of Latin epigraphy indicate a major reorganization of the workshop in the middle of the 1st century. The workshop ceased its activity in the following decade due to territorial reorganization under Roman influence and its distance from trade routes (Gorgues & Benavente Serrano, 2012). This workshop provides a context well-suited for investigating the technological choices related to ceramic firing in the Ebro Valley at the end of the Iron Age.

The ceramic material of the Mas de Moreno consists only of products known as Iberian painted/fine wares. It refers to a wheel thrown production, with a pink uniform colour and a dark red painted decor, with no temper visible to the naked eye and considered to be fired at high temperatures in an oxidizing atmosphere (Tarradell & Sanmarti, 1980 ; Mata & Bonet, 1992 ; Coll Conesa, 2000). Although Iberian fine wares present a significant technological uniformity (Tarradell & Sanmarti, 1980), the sampling was conducted in such a way that all types of pottery produced in the workshop were included in the study (non-Iberian types produced at the end of the workshop’s activity period were also sampled).

A number of fragments of unfired potteries were also found during the excavation of the workshop (Frerebeau, 2015b ; for a complete presentation of these unfired potsherds, see Frerebeau & Sacilotto, 2017). Of these, 11 samples have been analysed here (table 2).

Finally, 17 additional Iberian fine wares were sampled (table 2). These came from two settlements close to the workshop: Torre Cremada (Valdeltormo, Teruel, Aragon; 7 samples from the 1st century BC) and El Palao (Alcañiz, Teruel, Aragon; 10 samples dated between the 8th and the 4th century BC). Comparisons with these two settlements are not intended to establish genetic relationships (in a provenance meaning), but rather to propose a comparative technology study. Samples from El Palao and Torre Cremada have the same compositional ranges in the CaO-Al₂O₃-SiO₂ system and belong to the same category of Iberian fine wares as the material from Mas de Moreno (see below).

Table 2: Ceramic and clay (unfired pottery sherds) samples analyzed in this study. Phase 1 : 2nd century BC; Phase 2: first half of the 1st century BC; Phase 3: 50-30 BC. LOI: loss on ignition.

Sample	Material	Site	Phase	LOI (%)	CaO (%)	SiO2 (%)	Al2O3 (%)
BDX14914	clay	Mas de Moreno	2	19.48	17.17	51.16	20.66
BDX14917	clay	Mas de Moreno	2	18.76	17.17	51.34	20.89
BDX14918	clay	Mas de Moreno	2	18.91	17.33	51.10	20.69
BDX14920	clay	Mas de Moreno	2	18.52	16.52	51.66	21.09
BDX14921	clay	Mas de Moreno	2	18.32	16.50	51.90	20.97
BDX14922	clay	Mas de Moreno	2	20.69	21.32	48.31	19.70
BDX14924	clay	Mas de Moreno	2	18.64	16.78	51.66	20.85
BDX14925	clay	Mas de Moreno	2	18.53	16.66	51.33	20.84
BDX14926	clay	Mas de Moreno	2	19.92	19.63	49.39	19.35
BDX15030	clay	Mas de Moreno	2	19.99	19.33	50.61	19.93
BDX15031	clay	Mas de Moreno	2	20.59	20.62	49.91	19.37
BDX15032	ceramic	Mas de Moreno	1	13.15	13.92	53.68	19.69
BDX15033	ceramic	Mas de Moreno	1	14.87	15.15	53.45	19.22
BDX15034	ceramic	Mas de Moreno	1	13.31	17.58	51.62	19.04
BDX15035	ceramic	Mas de Moreno	1	12.98	15.16	52.94	19.21
BDX15036	ceramic	Mas de Moreno	1	13.76	15.87	50.00	19.99
BDX15037	ceramic	Mas de Moreno	1	6.76	16.38	49.64	21.14

BDX15038	ceramic	Mas de Moreno	1	7.78	15.15	52.72	19.97
BDX15040	ceramic	Mas de Moreno	1	14.78	14.70	54.09	20.65
BDX15041	ceramic	Mas de Moreno	1	11.35	16.11	50.56	20.38
BDX15042	ceramic	Mas de Moreno	1	14.40	14.14	54.00	20.45
BDX15043	ceramic	Mas de Moreno	1	14.79	14.39	52.94	20.19
BDX15044	ceramic	Mas de Moreno	1	10.93	17.50	52.22	18.10
BDX15045	ceramic	Mas de Moreno	1	10.80	19.14	52.34	16.76
BDX15053	ceramic	Mas de Moreno	1	8.89	14.60	53.52	20.75
BDX15054	ceramic	Mas de Moreno	1		14.34	50.41	21.31
BDX15445	ceramic	Mas de Moreno	2	5.57	16.43	50.15	19.82
BDX15446	ceramic	Mas de Moreno	2	13.96	19.83	49.35	19.53
BDX15448	ceramic	Mas de Moreno	2	13.54	15.68	52.04	21.01
BDX15449	ceramic	Mas de Moreno	2	12.03	17.48	50.81	20.57
BDX15450	ceramic	Mas de Moreno	2	6.83	16.92	51.69	20.86
BDX15451	ceramic	Mas de Moreno	2	9.41	20.37	49.07	19.39
BDX15452	ceramic	Mas de Moreno	2	8.11	16.53	51.68	20.92
BDX15453	ceramic	Mas de Moreno	2	7.17	17.35	51.16	20.27
BDX15457	ceramic	Mas de Moreno	2	5.81	15.92	50.69	21.56
BDX15461	ceramic	Mas de Moreno	2	9.86	16.23	51.53	19.81
BDX15464	ceramic	Mas de Moreno	2	5.10	16.84	51.39	20.09
BDX15465	ceramic	Mas de Moreno	2	7.40	17.08	50.16	19.63
BDX15466	ceramic	Mas de Moreno	2	7.16	15.35	52.10	19.85
BDX15468	ceramic	Mas de Moreno	2	12.26	17.00	52.12	20.20
BDX15473	ceramic	Mas de Moreno	2	16.71	16.25	51.87	19.45
BDX15640	ceramic	Mas de Moreno	3	7.05	16.94	50.04	20.16
BDX15641	ceramic	Mas de Moreno	3	15.19	16.93	52.48	19.51
BDX15643	ceramic	Mas de Moreno	3	10.97	19.50	49.45	19.79
BDX15644	ceramic	Mas de Moreno	3		18.30	50.68	19.30
BDX15647	ceramic	Mas de Moreno	3	6.36	16.20	52.81	20.17
BDX15649	ceramic	Mas de Moreno	3	6.54	16.10	51.49	21.05
BDX15651	ceramic	Mas de Moreno	3	8.26	18.02	50.73	19.31
BDX15652	ceramic	Mas de Moreno	3	6.73	16.06	50.34	21.14
BDX15653	ceramic	Mas de Moreno	3	5.85	14.30	51.80	21.46
BDX15654	ceramic	Mas de Moreno	3	5.80	15.04	50.93	21.66
BDX15659	ceramic	Mas de Moreno	3	9.28	15.77	50.14	21.32
BDX15660	ceramic	Mas de Moreno	3	5.53	17.81	49.44	20.46
BDX15661	ceramic	Mas de Moreno	3	6.84	16.32	49.90	21.13
BDX15662	ceramic	Mas de Moreno	3	9.21	16.56	50.21	20.49
BDX15663	ceramic	Mas de Moreno	3	5.77	12.84	54.48	21.15
BDX15664	ceramic	Mas de Moreno	3	3.52	16.25	50.42	20.93
BDX15665	ceramic	Mas de Moreno	3	7.37	15.95	50.52	21.23
BDX15666	ceramic	Mas de Moreno	3	6.09	13.93	52.74	22.73
BDX15668	ceramic	Mas de Moreno	3	4.92	16.08	49.89	21.08
BDX15669	ceramic	Mas de Moreno	3	8.19	14.78	51.93	21.25
BDX15671	ceramic	Torre Cremada		5.65	13.98	53.53	18.97
BDX15673	ceramic	Torre Cremada		4.87	11.52	56.58	19.73
BDX15674	ceramic	Torre Cremada		3.41	13.31	53.76	22.11
BDX15675	ceramic	Torre Cremada		7.26	8.83	57.18	16.07
BDX15676	ceramic	Torre Cremada		7.70	14.82	53.21	20.02
BDX15679	ceramic	Torre Cremada		7.40	16.24	53.10	19.99

BDX15680	ceramic	Torre Cremada	6.28	15.99	51.92	21.02
BDX16441	ceramic	El Palao	12.76	21.77	46.47	13.70
BDX16443	ceramic	El Palao	16.48	28.79	42.71	13.85
BDX16444	ceramic	El Palao	3.15	7.64	60.41	18.47
BDX16445	ceramic	El Palao	7.87	14.49	50.96	19.61
BDX16446	ceramic	El Palao	14.01	22.46	46.63	13.74
BDX16447	ceramic	El Palao		14.42	54.69	16.83
BDX16449	ceramic	El Palao	5.78	14.95	52.08	19.67
BDX16451	ceramic	El Palao	11.27	12.30	53.23	19.84
BDX16452	ceramic	El Palao	10.82	15.18	52.47	18.50
BDX16453	ceramic	El Palao	8.48	16.93	50.69	19.09

2.2 Powder X-ray diffraction

The mineralogical composition of the samples was determined by X-ray powder diffraction. The outer surfaces of all the samples were mechanically removed prior to analysis. Then, approximately 1 g of material per sample was manually powdered in an agate mortar.

The data were collected using a D8 Advance (Bruker) diffractometer in Bragg-Brentano configuration operating at 1.6 kW (40 kV, 40 mA) and equipped with a copper anode source ($k_{\alpha 1} = 1.5406 \text{ \AA}$; the k_{β} ray was removed by a Ni-filter in the diffracted beam). An 8 mm anti-scattering slit was mounted in front of the LynxEye© CCD detector. The explored area covered the $3\text{-}70^\circ$ (2θ) range, with an angle step of 0.02° and a time step of 2 seconds (the sample was rotated during the analysis). The stability of the instrument was checked between different series of measurements by analyzing a standard (corundum crystal, NIST 1976).

All diffractograms were processed in the same way:

- $k_{\alpha 2}$ lines were stripped using penalized likelihood (De Rooi *et al.*, 2014).
- All diffractograms were checked for possible sample displacements due to inaccurate powder sample mounting and then shifted accordingly (using quartz as an internal standard).
- All diffractograms were realigned to a common angular scale using linear interpolation between data points.
- Baselines were estimated using iterative mean suppression (4S Peak Filling, Liland, 2015) and then removed (negative values due to baseline subtraction were replaced by zeros).
- Data points below 4° (2θ) and above 54° (2θ) were removed.

Finally, all the diffractograms were combined into a 87×2501 matrix where each row corresponds to a sample and each column corresponds to a 2θ position. Each cell contains the corresponding X-ray photon count.

2.3 Correspondence analysis

We will only briefly recall the main aspects of correspondence analysis, as a detailed review of its mathematical properties is beyond the scope of this article (Lebart *et al.*, 2006 ; for an in-depth discussion, see Greenacre, 2007).

Correspondence analysis (CA) is similar to principal component analysis (PCA) in that it allows describing the statistical relationships that can exist between individuals and variables. However, the concept of similarity between rows and columns is different. In CA, two rows (resp. columns) are close to each other if they associate with columns (resp. rows) in the same way. Unlike PCA, CA analyzes the differences between relative values and considers both individuals and variables at the same time. This allows for the projection of row and column points in the same coordinate space, so that the relative positions of one set of points provide the reading keys for interpreting the positions of the other set of points along the axes (Greenacre, 2007).

CA studies the inertia (i.e., the weighted sum of the χ^2 distances of each point to the centroid) to create orthogonal components so that a maximum of the total inertia is represented on the first component, a

maximum of the residual inertia on the second component, and so on until the last dimension. CA maximizes the correspondence between individuals and variables instead of maximizing the amount of variance explained by its reduced space.

CA is an effective method for the chronological seriation of archaeological assemblages (see Ihm, 2005 for an historical overview). The order of the rows and columns is given by the coordinates along one dimension of the CA space, assumed to account for temporal variation. The direction of temporal change within the correspondence analysis space is arbitrary: additional information is needed to determine the actual order in time. CA is not limited to chronological modelling but is widely used to find a possible arrangement (ordering) of individuals and variables along any gradient, i.e., any aspect that is expected to be related to the observed composition (be it temporal or environmental).

2.4 Computational environment

All the data processing and statistical analysis were performed with R version 4.3.2 (2023-10-31) (R Core Team, 2023) and the following packages: `alkahest` 1.1.0 (Frerebeau, 2023a), `car` 3.1.2 (Fox & Weisberg, 2019), `dimensio` 0.3.1 (Frerebeau, 2023c), `isopleuros` 1.0.0 (Frerebeau, 2023d), `khroma` 1.10.0 (Frerebeau, 2023e), `rxylib` 0.2.11 (Kreutzer & Johannes Friedrich, 2023). The R code is openly available in Frerebeau (2023b) and allows to replicate all the results presented below.

3 Results and discussion

3.1 Correspondence analysis

The results of the correspondence analysis of the diffractograms are presented in fig. 1. Only the data from the analysis of the samples from Mas de Moreno were used, including unfired ceramics and sherds. The data from El Palao and Torre Cremada were introduced into the analysis as supplementary individuals. These additional individuals do not contribute to the calculation of the correspondence analysis itself, but they are projected onto the existing analysis space to visualize their relationships with the original dataset.

The first two dimensions are sufficient to retain about 74% of the total inertia contained in the data (fig. 1A and B). Plotting the coordinates of the individuals shows an interesting pattern (fig. 1C). The upper quadrants each consist of a small group of closely located individuals, likely exhibiting high similarity to one another. The remaining samples are distributed in the lower quadrants.

fig. 2 shows the contribution of the different columns to the construction of the first two CA-axes. It is important to note that the analysis is performed on the diffractograms: a diffraction peak represents a range of 2θ positions, spanning multiple columns in the data matrix. Consequently, the columns that contribute the most to the construction of the first axis (with a contribution greater than 0.5) are associated with the following diffraction peaks: 21.94° (plagioclases), 26.64° (quartz), 27.76° (plagioclases), 27.90° (plagioclases), and 29.42° (calcite). Similarly, for the second axis, the columns that contribute the most are those corresponding to the peaks at 12.32° (phyllosilicate), 26.66° (quartz), and 31.36° (melilites).

The first plane of the analysis exhibits the characteristic Guttman effect, also known as the arch effect (fig. 1, 3). This effect is characterized by a strong nonlinear relationship between the second factor and the first factor. The Guttman effect typically arises when a single dominant latent variable is present (Lebart & Saporta, 2014). Interestingly, the samples located in the upper left quadrant of the correspondence analysis plot are linked to diffraction peaks that correspond to clay minerals and calcite (fig. 3A, 1D, 4). These samples are positioned opposite to the ones associated with the peaks of diopside and anorthite along axis 1. Conversely, the samples located in the two lower quadrants are linked to the peaks of quartz and the melilite series.

The Guttman effect arises from the unimodal distribution of observed variables along a gradient, suggesting the possibility of ordering these variables along the same gradient. Our results strongly suggest that the gradient under consideration is related to the firing process: the first axis represents the opposition between minerals present in the raw material and those formed during firing. These secondary minerals gradually

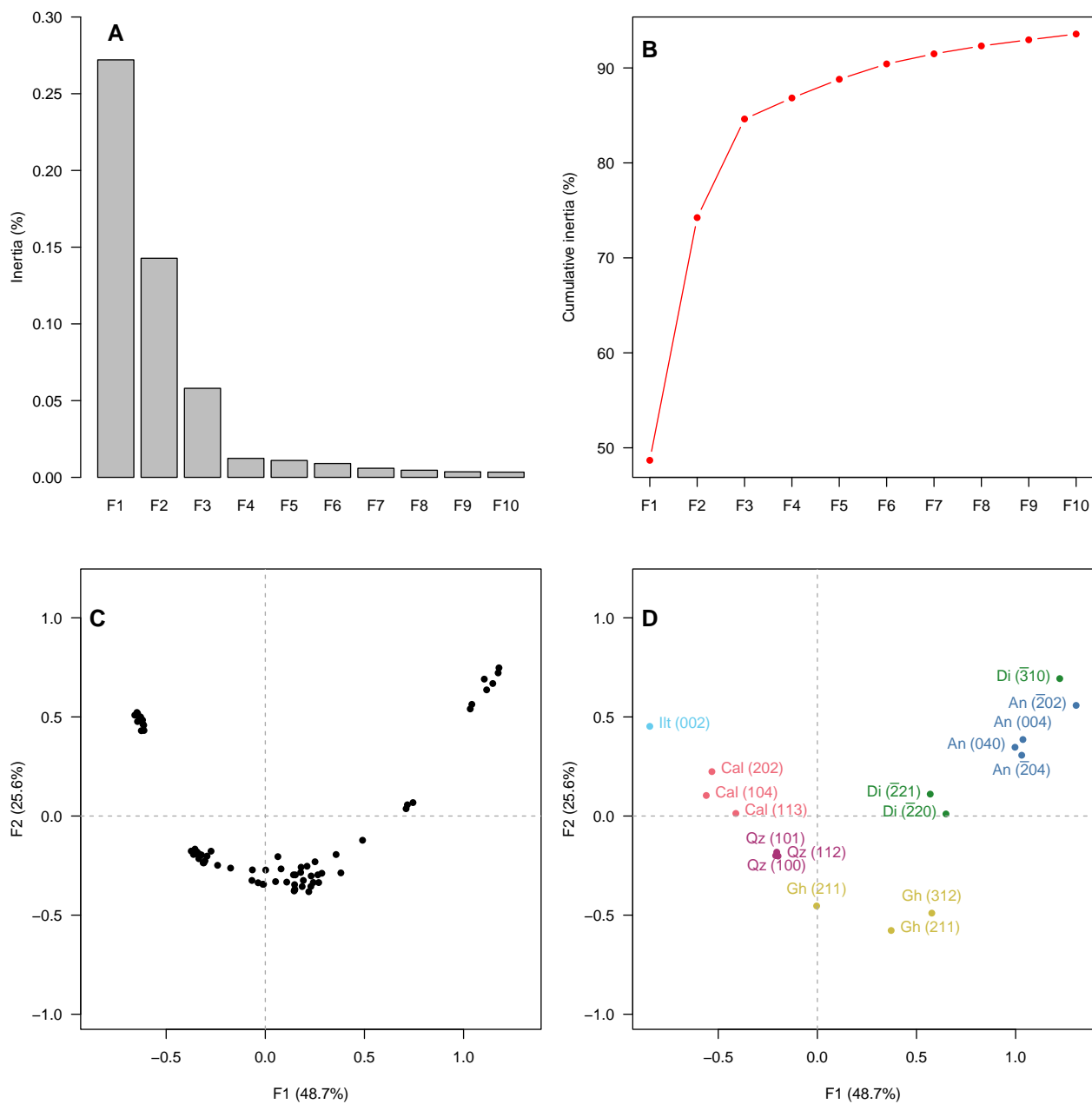


Figure 1: CA results of the XRD patterns of the Mas de Moreno samples. (A) Scree plot of inertia (only the first ten components are displayed). (B) Cumulative inertia of the first ten components. (C) CA rows score plot. (D) CA columns score plot, displaying only the main diffraction lines of a selected set of minerals of interest for improved readability. Ilt: illite; Cal: calcite; Qz: quartz; Gh: gehlenite; Di: diopside; An: anorthite.

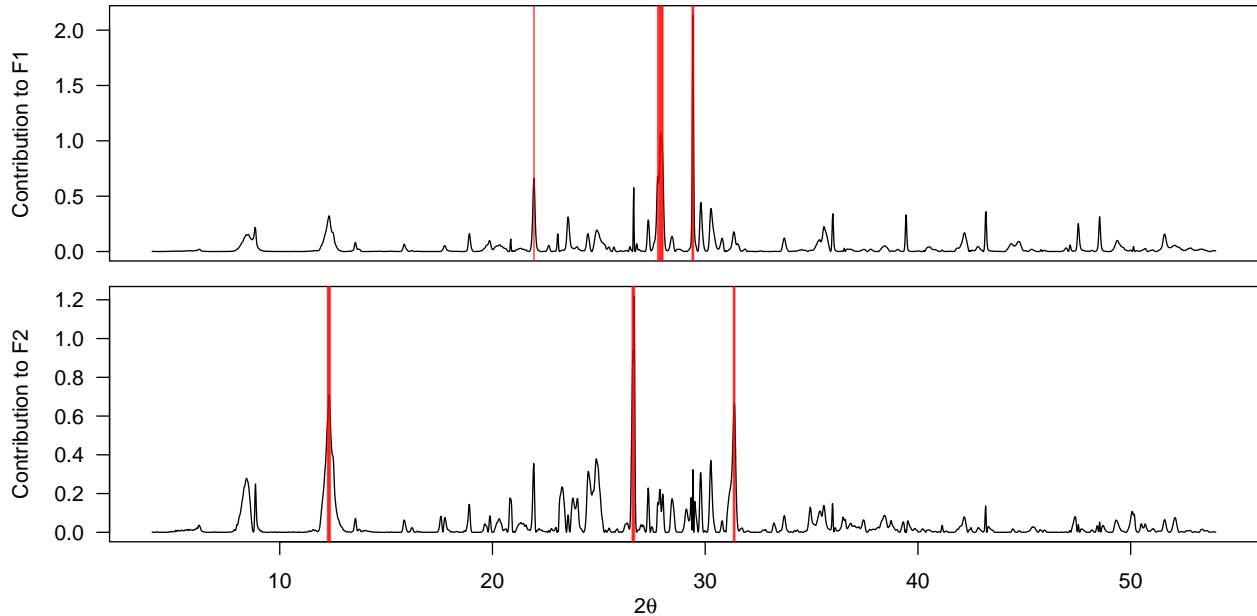


Figure 2: Columns contribution to the construction of the first two components. The twenty variables contributing the most to each component are highlighted in red.

form during the firing process as conditions change and are likely to be used in subsequent chemical reactions. Hence, a unimodal distribution can be expected for various 2θ positions along this gradient.

3.2 Ceramic firing

The production of ceramic materials involves solid-state transformations where the mineralogical composition of the final product differs from that of the raw material (Heimann, 1989). This is particularly true for Ca-rich ceramics, where the formation of new Ca-silicates can occur. The energy required for these transformations is supplied in the form of heat during firing, without reaching melting. As a result, the transformation process tends toward thermodynamic equilibrium but never fully achieves it (Grapes, 2010). One of the reasons for this deviation from equilibrium lies in the control exerted by reaction kinetics during ceramic firing (Treiman & Essene, 1983 ; Heimann, 1989 ; Heimann & Maggetti, 2019). The majority of archaeological ceramic materials are characterized by frozen-in phase transitions (Tsuchiyama, 1983 ; Rocabois *et al.*, 2001 ; Heimann & Maggetti, 2019).

Archaeological ceramic thus constitute highly heterogeneous materials, allowing for the existence of micro-equilibria confined to the reaction interfaces between grains. These micro-equilibria can result in the formation of thermodynamically incompatible mineral phases at the system scale (Maggetti, 1986 ; Heimann & Maggetti, 2019). However, the appearance of new phases is dependent on the availability of reactive components, which delays the initiation of these transformations compared to situations described by phase diagrams. Numerous studies have investigated these transformations (see, for instance, Peters & Iberg, 1978 ; Dondi *et al.*, 1998 ; Duminuco *et al.*, 1998 ; Riccardi *et al.*, 1999 ; Cultrone *et al.*, 2001 ; Rathossi & Pontikes, 2010), we only highlight the main findings in this context.

- During the firing process, the dehydroxylation of clay minerals and the thermal decomposition of calcium carbonates facilitate the availability of highly reactive oxides, enabling the formation of new phases, whether crystalline or not.
- At the interface between quartz and phyllosilicates, the dehydroxylation of phyllosilicates leads to the expected formation of potassium feldspars and aluminosilicates (mullite). Similarly, the interaction between dolomite and quartz is likely to result in the appearance of diopside. Furthermore, the contact between calcite and quartz is expected to produce wollastonite, which appears to be an intermediate

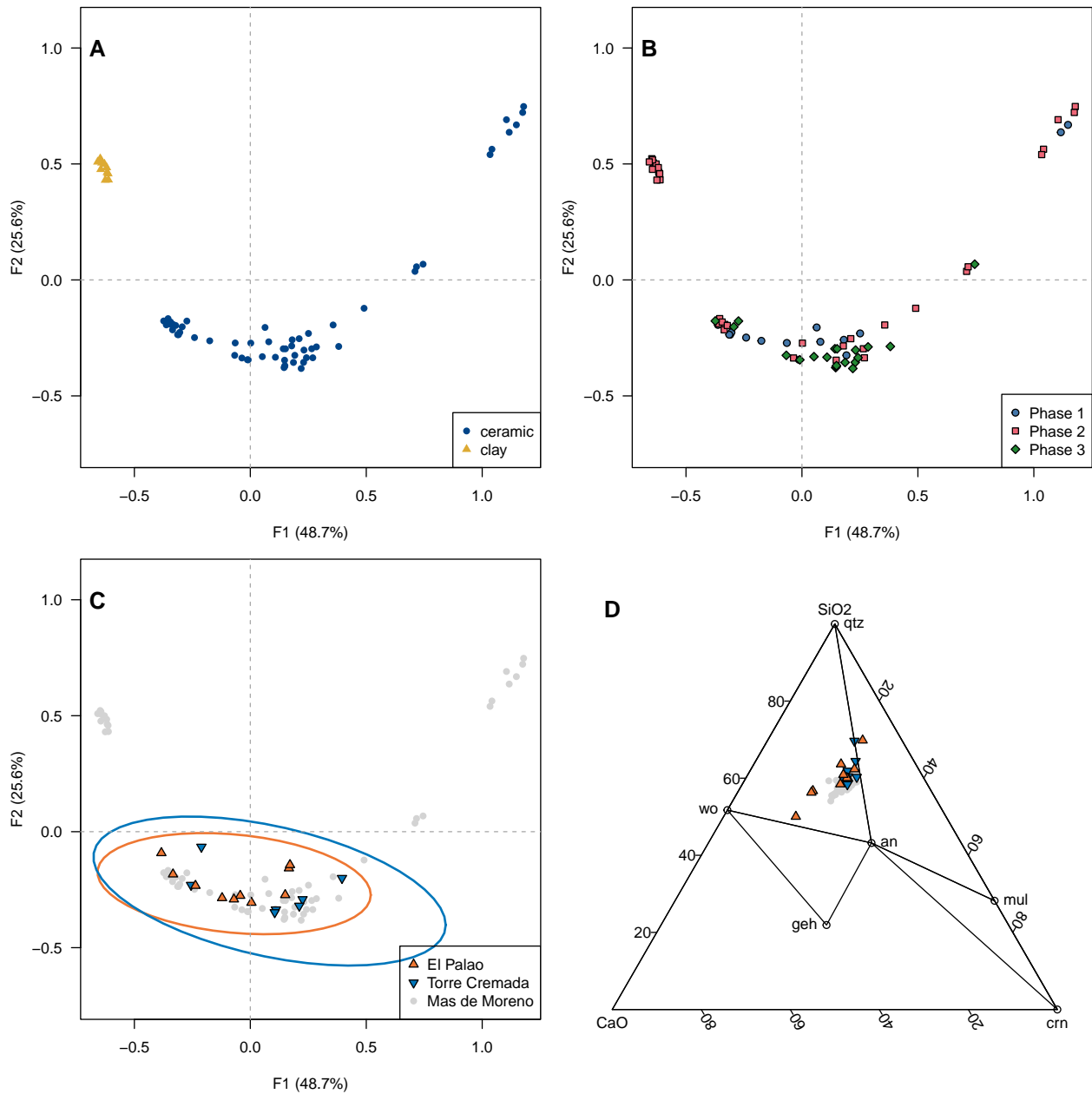


Figure 3: Guttman effect observed on the first plane of correspondence analysis: row coordinates are highlighted based on material (A), chronological phase (B), and supplementary individuals with 95% probability ellipses (C). CaO-SiO₂-Al₂O₃ ternary plot of the ceramic samples (D). Qz: quartz; Gh: gehlenite; An: anorthite; Wo: wollastonite; mul: mullite; crn: corundum. Data from Frerebeau (2015a) and Frerebeau (2015b).

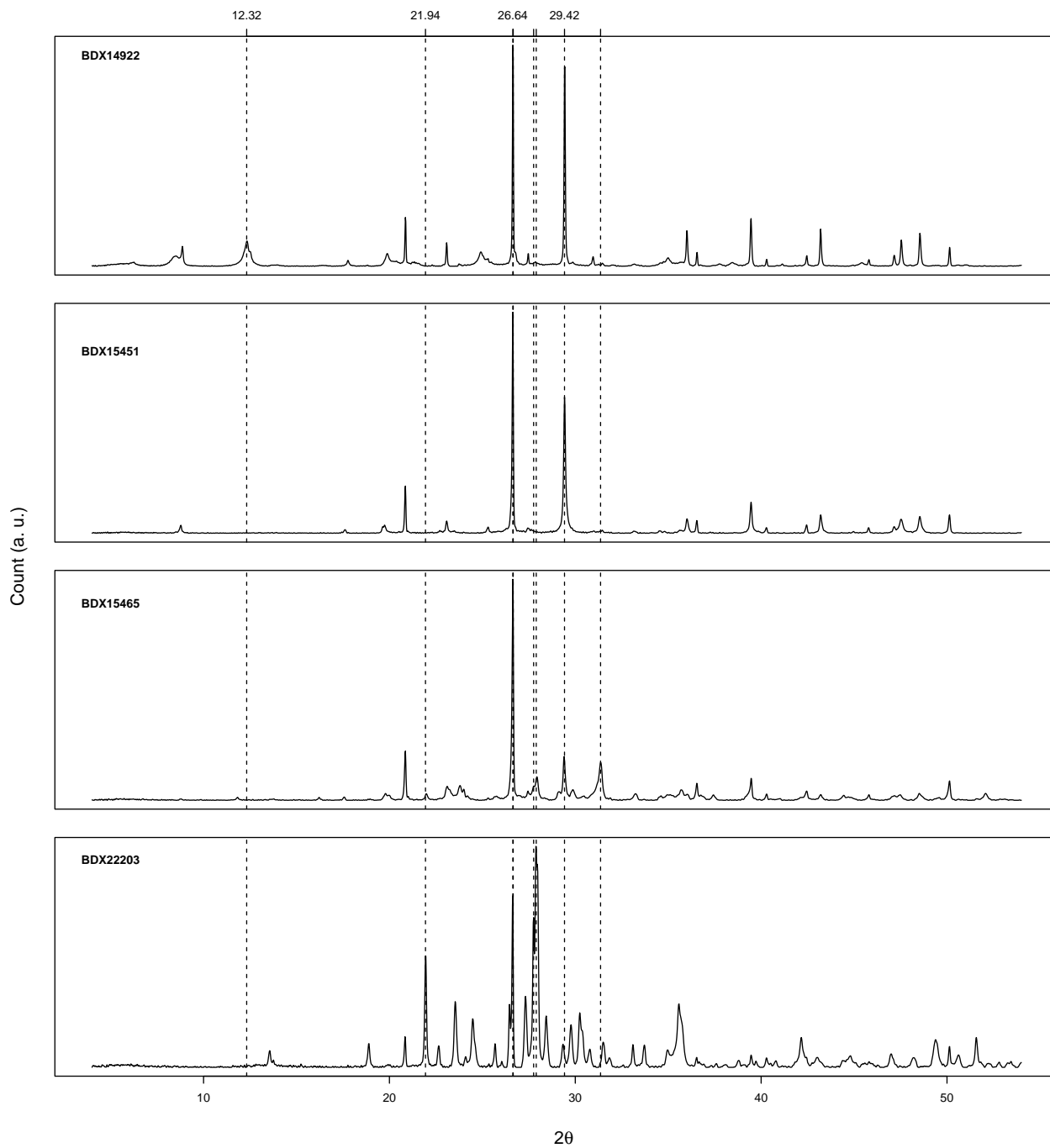


Figure 4: Diffractograms of representative samples from each quadrant of the CA plot (see fig. 1). From top to bottom: upper left quadrant (BDX14922), lower left quadrant (BDX15451), lower right quadrant (BDX15465), upper right quadrant (BDX22203). Only the peaks that contribute the most to the construction of the first two CA axes are indexed (see text and fig. 2).

reaction promoting the formation of anorthite (Traoré *et al.*, 2000).

- The interface between calcite, quartz, and phyllosilicates is anticipated to yield different calcium silicates (gehlenite, anorthite, wollastonite, and pyroxenes), sometimes accompanied by phases associated with the dehydroxylation of clay minerals, particularly potassium feldspars. The formation of gehlenite is a phenomenon that is accentuated by local enrichment in CaO.

The principal axis of correspondence analysis is built upon the opposition between primary phases and secondary phases. The resulting projection highlights the progression of firing, in accordance with the expected mineralogical transformations (fig. 1D). The intermediate position of gehlenite can also be explained. The ceramics from Mas de Moreno all belong to the category of Ca-rich ceramics, as defined by Noll (1991 ; Frerebeau *et al.*, 2020): within the CaO-Al₂O₃-SiO₂ system, they fall within the quartz-anorthite-wollastonite triangle (fig. 3D). In this case, the formed gehlenite is metastable. It serves as an intermediate product towards the formation of anorthite and wollastonite, linked to the diffusion of calcium through the matrix (Traoré *et al.*, 2000 ; Traoré *et al.*, 2003). As gehlenite forms a solid solution with akermanite (the melilite series), it can also promote the crystallization of diopside (primarily of the fassaite type) rather than anorthite (Dondi *et al.*, 1998 ; Rathossi & Pontikes, 2010).

Interestingly, figure 5 (top) illustrates the relationship between the first axis of the correspondence analysis and the loss on ignition (LOI) of the samples (see Frerebeau *et al.*, 2020 for the LOI data). It is observed that the LOI is inversely correlated with the coordinates of the individuals along the first axis. To further explore this relationship, a second-order polynomial regression analysis was conducted. The results indicated that the overall regression was statistically significant (RSE = 1.47 on 65 degrees of freedom, R² = 0.94, adjusted R² = 0.93, F(2, 65) = 482.7, p < 0.001), indicating a good fit of the polynomial regression model to the data.

Therefore, it appears that the ceramics from Mas de Moreno can be ordered according to the progress of these mineralogical transformations or, equivalently, according to the energy received during the firing (fig. 5, bottom).

3.3 Archaeological implications

The material from the Mas de Moreno is the result of waste from the production process. It is therefore necessary to distinguish between what is representative of material produced in the workshop and what is the result of a non-desirable situation leading to deliberate rejection (firing defect). In order to explore these two hypotheses, the diffractograms of several artifacts from consumption contexts (El Palao and Torre Cremada) were introduced into the previous analysis as supplementary individuals. This was made possible by the technical homogeneity of the material studied. Samples from El Palao and Torre Cremada have the same compositional ranges (fig. 3D) and belong to the same category of Iberian fine wares as the material from Mas de Moreno.

These additional individuals are all situated in the lower section of the first plane of the correspondence analysis (fig. 3C). This enables the differentiation of the artifacts from Mas de Moreno into those associated with regular production and those linked to misfiring (i.e., individuals located in the upper right quadrant; fig. 3A, 1D, 5 bottom). Individuals reflecting a typical production pattern exhibit peaks related to gehlenite rather than anorthite and diopside. This suggests a certain level of control over the energy input during firing to allow the development of this intermediate phase.

The firing process must be carefully controlled to maintain a favorable balance between benefits and risks throughout production. In the context of Iberian ceramics, the management of thermal parameters is primarily understood as a strategy to utilize calcareous materials without the risk of lime blowing (Petit-Domínguez *et al.*, 2003 ; Cultrone *et al.*, 2011 ; Cultrone *et al.*, 2014). However, the thermal decomposition of calcium carbonates is a necessary process to achieve the desired characteristics, especially aesthetic qualities.

By incorporating iron, the formation of calcium silicates during firing limits the development of coloration induced by the presence of iron oxides in the matrix. This occurs because iron can be integrated into amorphous or crystalline phases through substitution, rather than remaining as free oxides, thereby affecting its chromogenic properties. The cations Fe²⁺ and Fe³⁺ are incorporated into pyroxenes (preferably in octahedral coordination) through solid-state diffusion, replacing Mg²⁺ and Ca²⁺ ions, or into melilite-group

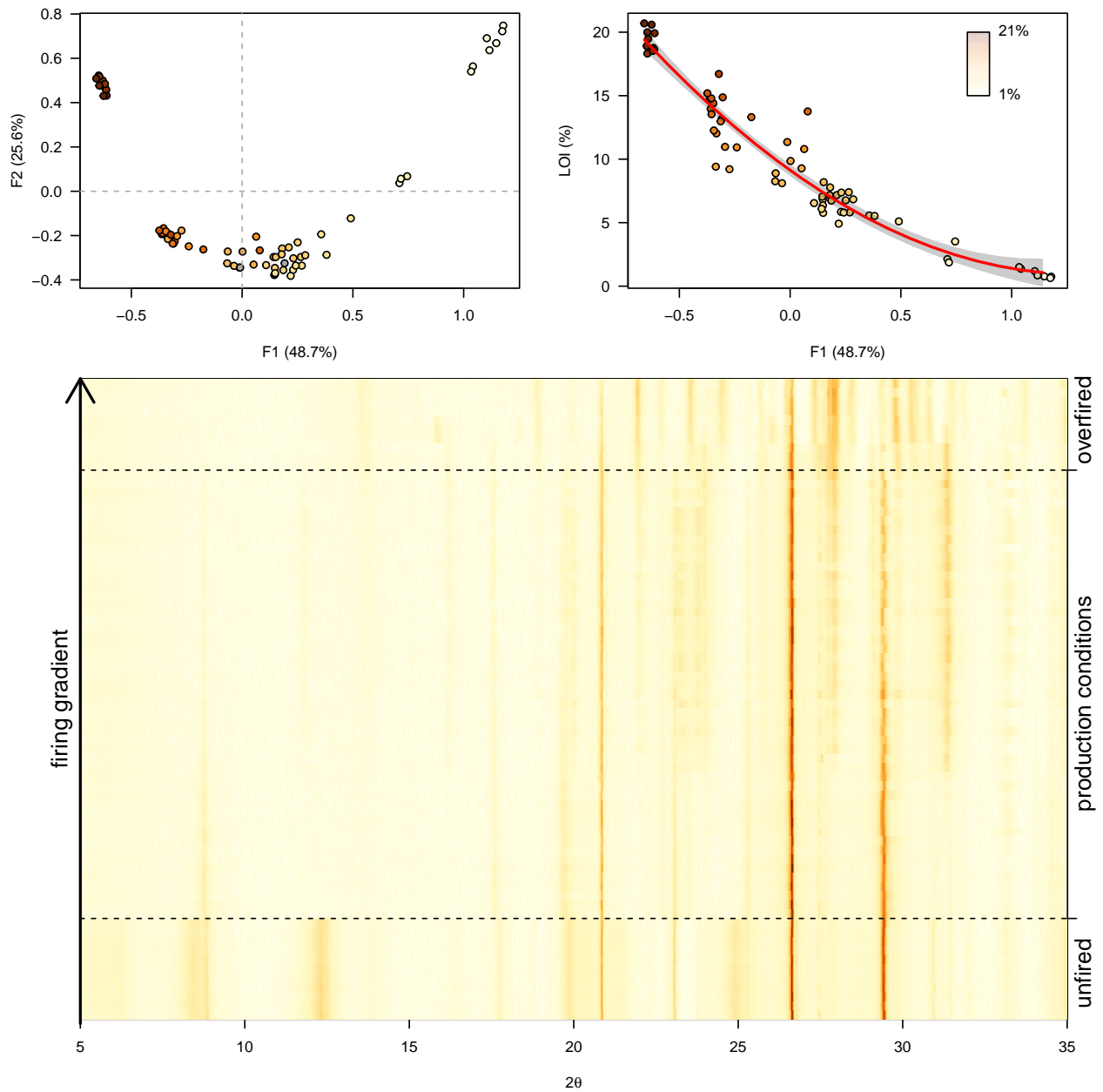


Figure 5: Top: the relationship between loss on ignition (LOI) and CA coordinates is depicted. The red line represents the second-order polynomial fit with an associated 95% confidence interval. Bottom: a heat map of the diffractograms in the 5-35° range (2θ) is displayed. The samples are ordered based on the first axis of the correspondence analysis. To enhance visualization, a square root transformation was applied.

phases (in tetrahedral coordination). This process prevents the formation of spinel compounds (Vedder & Wilkins, 1969 ; Nodari *et al.*, 2007) and plays a fundamental role in the manufacturing process of Iberian ceramics, as it allows for the attainment of a characteristic pink-colored surface.

Finally, it is worth noting that there appears to be no relationship with chronology (3B). Despite significant workshop modifications, including the adoption of a large amphora kiln that resulted in a shift in production quantities during the final years of the workshop's operation (Gorgues & Benavente Serrano, 2012), the produced artefacts exhibit consistent mineralogical characteristics.

4 Conclusion

The initial application of correspondence analysis to X-ray powder diffraction data of ceramic materials revealed the significant potential of this statistical method in the technological analysis of ancient pottery. The main advantage is the possibility of ordering a large number of samples according to a firing gradient. This allows for the tracking of mineralogical transformations occurring during firing and facilitates more precise comparisons than those based on estimating the equivalent firing temperature. Furthermore, this method enables the construction of calibration data sets from workshops, which can then be utilized to assess the firing of materials discovered in specific contexts.

However, a number of limitations need to be highlighted. Firstly, this method only allows us to obtain a relative order, without being able to identify any gaps in the sequence. Secondly, this approach relies on homogeneity conditions and mathematical assumptions that can be derived from the conditions formulated by Dunnell (1970) for chronological seriation. The homogeneity conditions state that all the groups included in such a study must: (1) be of comparable raw materials, (2) belong to the same technological tradition, (3) show mineralogical transformations related to firing. The mathematical assumptions state that the distribution of any mineralogical class is continuous through firing and exhibits the form of a unimodal curve. This last point is undoubtedly the most delicate, as many diffraction angles are paired with several minerals. Moreover, diffraction patterns depend not only on the mineralogical composition of the samples, but also on instrumental settings and counting statistics, which currently prevents the reuse of data acquired under different conditions.

These constraints will serve as a guide for future work. One of the next steps will be to work on variable selection. The use of whole diffractograms leads to the construction of a data matrix which tend to be sparse (a large portion of entries consists of zeros) and there is much redundant information. Finally, the use of resampling methods, such as bootstrapped approaches, should improve the stability of relative orderings, as shown by Peeples & Schachner (2012).

5 Acknowledgements

This study has received a State financial support managed by the French Agence Nationale de la Recherche under the program *Investissements d'avenir* (ANR-10-LABX-52).

The author is grateful to Alexis Gorgues (UMR 5607 Institut Ausonius) and José Antonio Benavente (Consortio Patrimonio Ibérico de Aragón) for providing access to archaeological material.

6 Data availability statement

The data that support the findings of this study are openly available in Frerebeau (2015a), Frerebeau (2015b), Frerebeau (2015c), Frerebeau (2015d).

The R code for data cleaning and analysis is openly available as a compendium in Frerebeau (2023b). It allows to replicate all the results presented above.

Colophon

This report was generated on 2024-01-11 16:51:11.592082 using the following computational environment and dependencies:

```
#> R version 4.3.2 (2023-10-31)
#> Platform: x86_64-pc-linux-gnu (64-bit)
#> Running under: Ubuntu 22.04.3 LTS
#>
#> Matrix products: default
#> BLAS: /usr/lib/x86_64-linux-gnu/blas/libblas.so.3.10.0
#> LAPACK: /usr/lib/x86_64-linux-gnu/lapack/liblapack.so.3.10.0
#>
#> locale:
#> [1] LC_CTYPE=fr_FR.UTF-8      LC_NUMERIC=C
#> [3] LC_TIME=fr_FR.UTF-8       LC_COLLATE=fr_FR.UTF-8
#> [5] LC_MONETARY=fr_FR.UTF-8   LC_MESSAGES=fr_FR.UTF-8
#> [7] LC_PAPER=fr_FR.UTF-8     LC_NAME=C
#> [9] LC_ADDRESS=C             LC_TELEPHONE=C
#> [11] LC_MEASUREMENT=fr_FR.UTF-8 LC_IDENTIFICATION=C
#>
#> time zone: Europe/Paris
#> tzcode source: system (glibc)
#>
#> attached base packages:
#> [1] stats      graphics  grDevices  utils      datasets  methods    base
#>
#> loaded via a namespace (and not attached):
#> [1] vctrs_0.6.2      dimensio_0.3.1  cli_3.6.1      knitr_1.43
#> [5] rlang_1.1.1     xfun_0.39      highr_0.10     car_3.1-2
#> [9] generics_0.1.3  glue_1.6.2     colorspace_2.1-0 rprojroot_2.0.3
#> [13] htmltools_0.5.5 fansi_1.0.4     scales_1.2.1   rmarkdown_2.21
#> [17] grid_4.3.2      abind_1.4-5    carData_3.0-5  evaluate_0.21
#> [21] munsell_0.5.0   tibble_3.2.1   fastmap_1.1.1  yaml_2.3.7
#> [25] lifecycle_1.0.3 bookdown_0.37  compiler_4.3.2 dplyr_1.1.2
#> [29] pkgconfig_2.0.3 here_1.0.1     isopleuros_1.0.0 rstudioapi_0.14
#> [33] khroma_1.10.0  digest_0.6.31  R6_2.5.1      tidyselect_1.2.0
#> [37] utf8_1.2.3     pillar_1.9.0   magrittr_2.0.3 tools_4.3.2
#> [41] gtable_0.3.3   ggplot2_3.4.2
```

References

- Coll Conesa, J., 2000. Aspectos de tecnología de producción de la cerámica ibérica. *SAGVNTVM-PLAV*, 3 : 191-209.
- Cultrone, G., Molina, E., Arizzi, A., 2014. The Combined Use of Petrographic, Chemical and Physical Techniques to Define the Technological Features of Iberian Ceramics from the Canto Tortoso Area (Granada, Spain). *Ceramics International*, 40, 7 : 10803-10816. DOI : 10.1016/j.ceramint.2014.03.072.
- Cultrone, G., Molina, E., Grifa, C., Sebastián, E., 2011. Iberian Ceramic Production From Basti (Baza, Spain): First Geochemical, Mineralogical and Textural Characterization. *Archaeometry*, 53, 2 : 340-363. DOI : 10.1111/j.1475-4754.2010.00545.x.
- Cultrone, G., Rodriguez-Navarro, C., Sebastian, E., Cazalla, O., De La Torre, M. J., 2001. Carbonate and Silicate Phase Reactions during Ceramic Firing. *European Journal of Mineralogy*, 13, 3 : 621-634. DOI : 10.1127/0935-1221/2001/0013-0621.
- de la Villa, R. V., García Giménez, R., Petit Domínguez, M. D., Rucandio, M. I., 2003. Physicochemical and Chemometric Characterisation of Late Roman Amphorae from Straits of Gibraltar. *Microchimica Acta*, 142 : 115-122. DOI : 10.1007/s00604-002-0955-z.
- De Rooi, J. J., Van Der Pers, N. M., Hendrikx, R. W. A., Delhez, R., Böttger, A. J., Eilers, P. H. C., 2014. Smoothing of X-ray Diffraction Data and Ka2 Elimination Using Penalized Likelihood and the Composite Link Model. *Journal of Applied Crystallography*, 47, 3 : 852-860. DOI : 10.1107/S1600576714005809.
- Dondi, M., Ercolani, B., Fabbri, B., Marsigli, M., 1998. An Approach to the Chemistry of Pyroxenes Formed during the Firing of Ca-rich Silicate Ceramics. *Clay Minerals*, 33, 3 : 443-452. DOI : 10.1180/000985598545741.
- Duminuco, P., Messiga, B., Riccardi, M. P., 1998. Firing Process of Natural Clays. Some Microtextures and Related Phase Compositions. *Thermochimica Acta*, 321, 1-2 : 185-190. DOI : 10.1016/S0040-6031(98)00458-4.
- Dunnell, R. C., 1970. Seriation Method and Its Evaluation. *American Antiquity*, 35, 03 : 305-319. DOI : 10.2307/278341.
- Fox, J., Weisberg, S., 2019. *An R Companion to Applied Regression*. Sage, Thousand Oaks CA.
- Frerebeau, N., 2015a. WDXRF Analysis of Iberian Potsherds from the Late Iron Age. Zenodo. URL : <https://doi.org/10.5281/zenodo.2594967>. DOI : 10.5281/zenodo.2594967.
- 2015b. WDXRF Analysis of Iberian Unfired Potsherds from the Late Iron Age. Zenodo. URL : <https://doi.org/10.5281/zenodo.1414297>. DOI : 10.5281/zenodo.1414297.
- 2015c. XRD Analysis of Iberian Potsherds from the Late Iron Age. Zenodo. DOI : 10.5281/zenodo.7947800.
- 2015d. XRD Analysis of Iberian Unfired Potsherds from the Late Iron Age. Zenodo. DOI : 10.5281/zenodo.7947821.
- 2023a. *alkahest: Pre-Processing XY Data from Experimental Methods*. Université Bordeaux Montaigne, Pessac, France. DOI : 10.5281/zenodo.7081524.
- 2023b. Compendium of R code and data for "Assessing the Firing of Ceramic Materials: a Seriation-Based Approach". Compendium. Université Bordeaux Montaigne, Pessac. URL : <https://github.com/nfrerebeau/FiringSeriation>. DOI : 10.5281/zenodo.8020137.
- 2023c. *dimensio: Multivariate Data Analysis*. Université Bordeaux Montaigne, Pessac, France. DOI : 10.5281/zenodo.4478530.
- 2023d. *isopleuros: Ternary Plots*. Université Bordeaux Montaigne, Pessac, France.
- 2023e. *khroma: Colour Schemes for Scientific Data Visualization*. Université Bordeaux Montaigne, Pessac, France. DOI : 10.5281/zenodo.1472077.
- Frerebeau, N., Ben Amara, A., Cantin, N., 2020. Analyse de données de composition et identification des altérations géochimiques des matériaux céramiques : le cas des productions d'un atelier ibérique (Teruel, Espagne ; IIe-Ier siècles avant J.-C.). *ArcheoSciences, revue d'Archéométrie*, 44, 1 : 33-50. DOI : 10.4000/archeosciences.7220.
- Frerebeau, N., Pernot, M., 2018. Dans la chaleur des fours : que restituer des pratiques des céramistes des sociétés anciennes ? *ArcheoSciences, revue d'Archéométrie*, 42, 2 : 95-105. DOI : 10.4000/archeosciences.6007.
- Frerebeau, N., Sacilotto, C., 2017. On Some Iberian Unfired Pottery Sherds from the Late Iron Age (Second Century BC). In Gorgues, A., Rebay-Salisbury, K., Salisbury, R. B. (dir.). *Material Chains in Late Prehistoric Europe and the Mediterranean – Time, Space and Technologies of Production*. Mémoires 48. Ausonius Éditions, Bordeaux.
- Garciajimenez, R., Vigildelavilla, R., Petitdominguez, M., Rucandio, M., 2006. Application of Chemical, Physical and Chemometric Analytical Techniques to the Study of Ancient Ceramic Oil Lamps. *Talanta*, 68,

- 4 : 1236-1246. DOI : 10.1016/j.talanta.2005.07.033.
- Gorgues, A., Benavente Serrano, J. A., 2007. Les ateliers de potiers de Foz-Calanda (Teruel) aux IIe-Ier siècles avant notre ère. *Mélanges de la Casa de Velázquez*, 37, 1 : 295-312.
2012. Organisation du travail et technologie potière dans les ateliers ibériques tardifs du Mas de Moreno (Foz-Calanda, Teruel) : bilan provisoire des recherches (2005-2011). Actas del II Congreso Internacional (Alcañiz-Tivissa, 16-19 de noviembre de 2011). Iberos del Ebro. Documenta. Institut Català d'Arqueologia Clàssica, Tarragona.
- Gosselain, O. P., 1992. Bonfire of the Enquiries. Pottery Firing Temperatures in Archaeology: What For? *Journal of Archaeological Science*, 19, 3 : 243-259. DOI : 10.1016/0305-4403(92)90014-T.
- Grapes, R., 2010. *Pyrometamorphism*. Springer, Berlin Heidelberg. DOI : 10.1007/978-3-642-15588-8.
- Greenacre, M. J., 2007. *Correspondence Analysis in Practice*. Interdisciplinary Statistics Series. Chapman & Hall/CRC, Boca Raton.
- Heimann, R. B., 1989. Assessing the Technology of Ancient Pottery: The Use of Ceramic Phase Diagrams. *Archaeomaterials*, 3 : 123-148.
- Heimann, R. B., Maggetti, M., 2019. The Struggle between Thermodynamics and Kinetics: Phase Evolution of Ancient and Historical Ceramics. *The Contribution of Mineralogy to Cultural Heritage*. Mineralogical Society of Great Britain and Ireland. DOI : 10.1180/EMU-notes.20.6.
- Holakooei, P., Tessari, U., Verde, M., Vaccaro, C., 2014. A New Look at XRD Patterns of Archaeological Ceramic Bodies: An Assessment for the Firing Temperature of 17th Century Haft Rang Tiles from Iran. *Journal of Thermal Analysis and Calorimetry*, 118, 1 : 165-176. DOI : 10.1007/s10973-014-4012-z.
- Hubbard, C. R., Snyder, R. L., 1988. RIR - Measurement and Use in Quantitative XRD. *Powder Diffraction*, 3, 2 : 74-77. DOI : 10.1017/S0885715600013257.
- Ihm, P., 2005. A Contribution to the History of Seriation in Archaeology. In Wehls, C., Gaul, W. (dir.). Classification – the Ubiquitous Challenge. 28th Annual Conference of the Gesellschaft Für Klassifikation e.V., University of Dortmund, March 9-11, 2004. Springer, Berlin Heidelberg. DOI : 10.1007/3-540-28084-7_34.
- Kreutzer, S., Johannes Friedrich, 2023. *rxylib: Import XY-Data into R*.
- Lebart, L., Piron, M., Morineau, A., 2006. *Statistique exploratoire multidimensionnelle : Visualisations et inférences en fouilles de données*. Dunod, Paris.
- Lebart, L., Saporta, G., 2014. Historical Elements of Correspondence Analysis and Multiple Correspondence Analysis. In Blasius, J., Greenacre, M. (dir.). *Visualization and Verbalization of Data*. CRC Press - Taylor and Francis, Boca Raton. DOI : 10.1201/b16741-5.
- Lemonnier, P., 1983. L'Étude des systèmes techniques – Une urgence en technologie culturelle. *Techniques & culture*, 1 : 11-26.
- Liland, K. H., 2015. 4S Peak Filling – Baseline Estimation by Iterative Mean Suppression. *MethodsX*, 2 : 135-140. DOI : 10.1016/j.mex.2015.02.009.
- Livingstone Smith, A., 2001. Bonfire II: The Return of Pottery Firing Temperatures. *Journal of Archaeological Science*, 28, 9 : 991-1003. DOI : 10.1006/jasc.2001.0713.
- Maggetti, M., 1986. Majolika aus Mexiko - Ein archäometrische Fallbeispiel. *Fortschritte der Mineralogie*, 64 : 87-103.
- Maritan, L., Holakooei, P., Mazzoli, C., 2015. Cluster Analysis of XRPD Data in Ancient Ceramics: What For? *Applied Clay Science*, 114 : 540-549. DOI : 10.1016/j.clay.2015.07.016.
- Mata, C., Bonet, H., 1992. La cerámica ibérica ensayo de tipología. *Estudios de arqueología ibérica y romana : homenaje a Enrique Pla Ballester*. Serie de Trabajos Varios 89. Diputación Provincial de Valencia, Valencia.
- Nodari, L., Marcuz, E., Maritan, L., Mazzoli, C., Russo, U., 2007. Hematite Nucleation and Growth in the Firing of Carbonate-Rich Clay for Pottery Production. *Journal of the European Ceramic Society*, 27, 16 : 4665-4673. DOI : 10.1016/j.jeurceramsoc.2007.03.031.
- Noll, W., 1991. *Alte Keramiken und ihre Pigment – Studien zu Material und Technologie*. E. Schweizerbart'sche Verlagsbuchhandlung, Stuttgart.
- Peeples, M. A., Schachner, G., 2012. Refining Correspondence Analysis-Based Ceramic Seriation of Regional Data Sets. *Journal of Archaeological Science*, 39, 8 : 2818-2827. DOI : 10.1016/j.jas.2012.04.040.
- Peters, T., Iberg, R., 1978. Mineralogical Changes During Firing of Calcium-Rich Brick Clays. *American Ceramic Society Bulletin*, 57, 5 : 503-509.
- Petit-Domínguez, M. D., García-Giménez, R., Rucandio, M. I., 2003. Chemical Characterization of Iberian Amphorae and Tannin Determination as Indicative of Amphora Contents. *Microchimica Acta*, 141, 1-2 :

63-68. DOI : 10.1007/s00604-002-0930-8.

Piovesan, R., Dalconi, M. C., Maritan, L., Mazzoli, C., 2013. X-Ray Powder Diffraction Clustering and Quantitative Phase Analysis on Historic Mortars. *European Journal of Mineralogy*, 25, 2 : 165-175. DOI : 10.1127/0935-1221/2013/0025-2263.

R Core Team, 2023. *R: A Language and Environment for Statistical Computing*. R Foundation for Statistical Computing, Vienna, Austria.

Rathossi, C., Pontikes, Y., 2010. Effect of Firing Temperature and Atmosphere on Ceramics Made of NW Peloponnese Clay Sediments. Part I: Reaction Paths, Crystalline Phases, Microstructure and Colour. *Journal of the European Ceramic Society*, 30, 9 : 1841-1851. DOI : 10.1016/j.jeurceramsoc.2010.02.002.

Riccardi, M., Messiga, B., Duminuco, P., 1999. An Approach to the Dynamics of Clay Firing. *Applied Clay Science*, 15, 3-4 : 393-409. DOI : 10.1016/S0169-1317(99)00032-0.

Rietveld, H. M., 1969. A Profile Refinement Method for Nuclear and Magnetic Structures. *Journal of Applied Crystallography*, 2, 2 : 65-71. DOI : 10.1107/S0021889869006558.

Rocabois, P., Pontoire, J. N., Lehmann, J., Gaye, H., 2001. Crystallization Kinetics of Al₂O₃-CaO-SiO₂ Based Oxide Inclusions. *Journal of Non-Crystalline Solids*, 282, 1 : 98-109. DOI : 10.1016/S0022-3093(01)00332-5.

Shepard, A. O., 1936. The Technology of Pecos Pottery. In Kidder, A. V., Shepard, A. O. (dir.). *The Pottery of Pecos*. Papers of the Southwestern Expedition 7. Yale University Press, New Haven.

Tarradell, M., Sanmarti, E., 1980. L'état actuel des études sur la céramique ibérique. In Lévêque, P., Moret, P. (dir.). *Céramiques hellénistiques et romaines*. Annales Littéraires de l'Université de Besançon 242. Les Belles Lettres, Paris.

Tite, M. S., 1969a. Determination of the Firing Temperature of Ancient Ceramics by Measurement of Thermal Expansion. *Nature*, 222, 5188 : 81-81. DOI : 10.1038/222081a0.

1969b. Determination of the Firing Temperature of Ancient Ceramics by Measurement of Thermal Expansion: A Reassessment. *Archaeometry*, 11, 1 : 131-143. DOI : 10.1111/j.1475-4754.1969.tb00636.x.

1995. Firing Temperature Determinations – How and Why? In Lindahl, A., Stilborg, O. (dir.). The Aim of Laboratory Analyses of Ceramics in Archaeology. KVHAA Konferenser 34 (Lund, Sweden; 7-9 April 1995). Kungl. Vitterhets Historieoch Antikivitetets Akademien, Stockholm.

1999. Pottery Production, Distribution, and Consumption: The Contribution of the Physical Sciences. *Journal of Archaeological Method and Theory*, 6, 3 : 181-233. DOI : 10.1023/A:1021947302609.

Traoré, K., Kabré, T. S., Blanchart, P., 2000. Low Temperature Sintering of a Pottery Clay from Burkina Faso. *Applied Clay Science*, 17, 5-6 : 279-292. DOI : 10.1016/S0169-1317(00)00020-X.

2003. Gehlenite and Anorthite Crystallisation from Kaolinite and Calcite Mix. *Ceramics International*, 29, 4 : 377-383. DOI : 10.1016/S0272-8842(02)00148-7.

Treiman, A. H., Essene, J., 1983. Phase Equilibria in the System CaO-SiO₂-CO₂. *American Journal of Science*, 283-A : 97-120.

Tsuchiyama, 1983. Crystallization Kinetics in the System CaMgSi₂O₆-CaAl₂Si₂O₈: The Delay in Nucleation of Diopside and Anorthite. *American Mineralogist*, 68 : 687-698.

Vedder, W., Wilkins, R. W. T., 1969. Dehydroxylation and Rehydroxylation, Oxidation and Reduction of Micas. *American Mineralogist*, 54 : 482-509.